Oscillator-strength distributions for discrete and continuum transitions of excited states of cesium

Jayanti Lahiri
Department of Physics, Southern Technical Institute, Marietta, Georgia 30060

Steven T. Manson
Department of Physics and Astronomy, Georgia State Univeristy, Atlanta, Georgia 30303
(Received 2 December 1985)

Calculations of the photoionization cross sections of excited nl states of cesium for $n \leq 9$ and $l \leq 3$ have been carried out within the framework of the central-field model. In addition, oscillator strengths for discrete transitions among these excited states have been obtained. The oscillator-strength distributions are presented and analyzed and the prominent zeros in the matrix elements for excited states are discussed in detail. Procedures and pitfalls in interpolation and extrapolation of discrete oscillator strengths are discussed, and the photoelectron angular distributions from these excited states are also presented.

I. INTRODUCTION

The study of excited states of atoms allows one to investigate the phenomenology of physically large, yet relatively simple, systems. In addition, by scrutinizing ionizing transitions one has a probe of continuum wave functions far from the nucleus, a region inaccessible from ground states. Since continuum wave functions are, in general, the least understood element involved in theoretical descriptions of ionization, it is of great interest to study them.

The simplest ionization process is photoionization since the incident particle, the photon, disappears in the interaction. Furthermore, the progress of laser technology has made experimental measurements of photoionization of excited atoms with one or two lasers or a laser plus a synchrotron possible. Added to this is the fact that excited-state photoionization is of importance in hot regions such as stellar atmospheres and CTR plasmas, as well as being very helpful in understanding the inverse process, radiative recombination. Previous theoretical studies have uncovered several new phenomena in the photoionization of excited atoms, notably the existence of a number of zeros in the transition matrix elements, far more than are seen for ground-state atoms.[1-3] These zeros were predicted on the basis of simple central-field calculations, but more sophisticated Hartree-Fock calculations reveal exactly the same phenomenology.[4,5] This points out the utility of the central-field model, in view of its simplicity, to get an overview of systematics and to reveal areas for more detailed studies.

In this paper we focus on the photoionization of excited nl states of cesium, up to $n=9$ and $l=3$. Cesium was chosen because of its low ionization potential, making it attractive experimentally, the rich phenomenology, seen previously,[1-4] and the simplicity of the outer-shell structure, making it less likely that correlation effects are of great importance. Calculations of the photoionization cross sections and photoelectron angular distribution asymmetry parameters β were performed from threshold to 5 Ry above threshold in each case. Additionally, discrete oscillator strengths for the possible optically allowed transitions among the various excited states were obtained in order to study the optical oscillator-strength distribution both above and below threshold.

In Sec. II a brief review of the theory and calculational method is given. Section III presents and discusses our results for oscillator-strength distributions, photoionization cross sections, and photoelectron angular distributions. In addition, a discussion of interpolation in order to obtain oscillator strengths for $nl \rightarrow n'l'$ transitions where $n' > 9$ is presented. Section IV presents a summary, conclusions, and a prospectus for future work.

II. THEORY AND METHOD OF CALCULATION

Within the context of the central-field model, the cross section for photoionization of an nl atomic electron is given by[6]

$$\sigma_{nl}(\epsilon)=(4/3)\pi^2\alpha a_0^2\frac{N_{nl}}{2l+1}(\epsilon-\epsilon_{nl}) \times\{l[R_{l-1}(\epsilon)]^2+(l+1)[R_{l+1}(\epsilon)]^2\}\ , \quad (1)$$

where α is the fine-structure constant, a_0 is the Bohr radius, N_{nl} is the occupation number of the subshell, ϵ and ϵ_{nl} (intrinsically negative) are the photoelectron energy after and before the interaction, respectively, and

$$R_{l\pm1}(\epsilon)=\int_0^\infty P_{nl}(r)rP_{\epsilon,l\pm1}(r)dr \quad (2)$$

with $P_{nl}(r)/r$ and $P_{\epsilon l\pm1}(r)/r$ are the radial parts of the initial discrete and final continuum states. The discrete function is normalized to unity and the continuum to unit energy in rydbergs, i.e.,

$$P_{nl}(r)\rightarrow\pi^{-1/2}\epsilon^{-1/4}\sin[\epsilon^{1/2}r-\tfrac{1}{2}l\pi+\epsilon^{-1/2}\ln 2\epsilon^{1/2}r+\sigma_l(\epsilon)+\delta_l(\epsilon)] \text{ as } r\rightarrow\infty \tag{3}$$

with $\sigma_l(\epsilon)$ the Coulomb phase shift and $\delta_l(\epsilon)$ the non-Coulomb phase shift.

The photoelectron angular distribution for unpolarized incident photons is given by[7]

$$\frac{d\sigma_{nl}}{d\Omega}=\frac{\sigma_{nl}}{4\pi}\left[1-\frac{\beta_{nl}(\epsilon)}{2}P_2(\cos\theta)\right], \tag{4}$$

where $P_2(x)=(3x^2-1)/2$ and the asymmetry parameter[8]

$$\beta_{nl}(\epsilon)=\frac{l(l-1)R_{l-1}^2+(l+1)(l+2)R_{l+1}^2-6l(l+1)R_{l-1}R_{l+1}\cos(\xi_{l+1}-\xi_{l-1})}{(2l+1)[lR_{l-1}^2+(l+1)R_{l+1}^2]} \tag{5}$$

with $\xi_l=\sigma_l+\delta_l$.

Hartree-Slater central-field wave functions[9] were used in this work. The potential appropriate to the ground state was employed to solve the single-particle Schrödinger equation for both the initial discrete and final continuum states. Thus, exchange was treated only approximately, and core relaxation was neglected.

III. RESULTS AND DISCUSSION

Calculated results for photoionization cross sections, discrete oscillator strengths, and photoelectron angular distributions of excited states of Cs are the principal focus of this work. Initial s, p, d, and f states with $n=6$–9, along with the excited $5d$, $4f$, and $5f$ states have been considered.

Owing to the lack of experimental photoionization cross sections for excited states of Cs, it is difficult to establish the accuracy of our results. On the other hand, some experimental and semiempirical work has been done on discrete oscillator strengths. Since the accuracy of the discrete and continuum wave functions should be comparable, comparison of our discrete oscillator strengths with available values gives some indication of the accuracy of our discrete wave functions and by inference, gives information on the reliability of the continuum wave function and photoionization cross sections.

Note that excited-state wave functions have an important qualitative difference from most ground-state wave functions in that a majority of their amplitude is in a region where the potential is purely Coulomb. Thus, for most of their extent, these wave functions are purely hydrogenic with a quantum defect (phase shift for continuum states) generated by the inner non-Coulomb region of the potential. For many matrix elements between two such wave functions, the contribution of the inner region is insignificant and the matrix element can be characterized by the quantum defects (phase shift) of each of the states. This, of course, is the philosophy behind the Bates-Damgaard analytic calculation of discrete oscillator strengths.[10] For this reason, along with the fact that phase shifts are crucial factors in photoelectron angular distributions, the calculated quantum defects and phase shifts are discussed first.

A. Quantum defects and phase shifts

For an atomic nl electron, the quantum defect μ_{nl} is related to the electron binding energy ϵ_{nl} by[11]

$$\epsilon_{nl}=\frac{R}{n-\mu_{nl}}, \tag{6}$$

where $R=13.6$ eV. This is the fundamental equation of quantum-defect theory.[11] μ_{nl} provides information about the inner non-Coulomb region of the potential. Its importance is enhanced by the fact that it varies very slowly with increasing n and rapidly approaches its asymptotic value μ_l. Furthermore, it provides a connection between discrete and continuum spectra[11] since the continuum phase shift at threshold, $\delta_l(0)=\pi\mu_l$.

Our calculated quantum-defect and phase-shift results are shown in Fig. 1, where it is seen that the s- and p-wave results drop monotonically starting in the discrete, the d wave starts increasing and reaches a maximum in the discrete, followed by a drop which continues for all higher energies, and the f wave is increasing in the discrete and exhibits a shape resonance just above threshold. These results can be understood in terms of the effective potentials, i.e., actual potential plus centrifugal potential, "seen" by each of the partial waves.[12] The s wave,

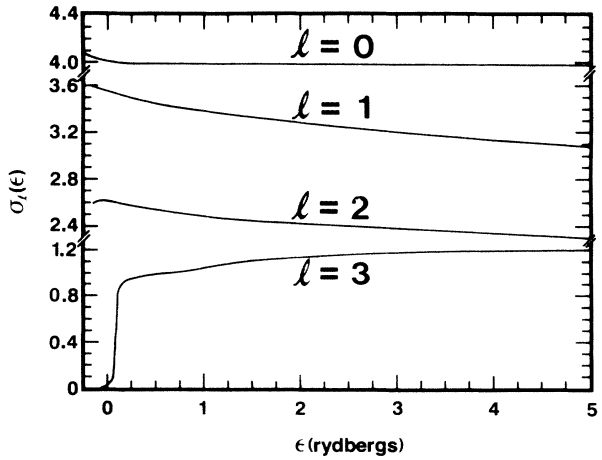

FIG. 1. Phase shifts (in units of π) and quantum defects (for $\epsilon<0$) for cesium.

having no potential barrier, and the p wave, which has only a weak centrifugal barrier at very short distances, are very penetrating orbitals, even for the lowest member of the discrete. Consequently, since increases in energy move the orbital even closer in, cancellation effects occur and the quantum defects and phase shifts decrease with increasing energy,[13] as seen in Fig. 1.

For the d wave, the effective potential has a rather different shape, with a larger centrifugal barrier near the nucleus and a double well with a barrier between them at the outer edge of the atom. This barrier results from the "competition" between the attractive electrostatic potential and repulsive centrifugal potential; in the case it is an "underwater" barrier, i.e., its height is below zero energy. This d-wave barrier is fairly weak, but it still manages to keep the lowest discrete d wave from penetrating completely. Going up in energy to higher discrete states the barrier penetration increases, thus increasing the quantum defect, as seen in Fig. 1. At energies above the barrier height, the d orbital is penetrating, and the quantum defect and phase shift decrease monotonically with energy.

The f-wave potential has a huge centrifugal barrier near the nucleus and a double well like the d wave, but with a much higher and broader barrier between them, about 0.5 Ry (positive energy) high.[12] Thus, f states with energy much below the barrier height are in the outer well primarily; they have very little amplitude in the inner region where the potential deviates from Coulomb. As a result, the quantum defects and phase shifts are close to zero. With increasing energy they do penetrate more, increasing the quantum defects in the discrete and the phase shifts in the continuum. As the energy reaches the top of the barrier, the wave function moves in to the inner barrier rather abruptly, giving rise to the shape resonance seen in Fig. 1.

TABLE I. Threshold phase shifts (asymptotic quantum defects) for cesium compared with experimental results from Ref. 14.

l	Experiment[a]	Theory
0	4.06	4.02
1	3.58	3.56
2	2.47	2.61
3	0.03	0.03

[a]Reference 14.

To get some idea of the accuracy of both the discrete and continuum wave functions, the calculated and experimental[14] asymptotic quantum defects are given in Table I. The agreement for s, p, and f waves is seen to be quite good; the d wave is somewhat less so, the theoretical value being a bit larger than the experimental. This means that the actual d-wave potential is less attractive than the theoretical. The reason that this shows up in the d wave, but no other, is due to the sensitivity of the barrier at the outer edge of the atom. Since the barrier results from a difference of two large numbers, a small error in one of them could lead to a large error in the difference. The comparison of Table I suggests that the actual barrier is higher than our calculation predicts. Thus, it is clear that the d-wave functions used in this calculation are slightly too compact.

B. Discrete oscillator strengths

Oscillator strengths for absorption among the ground $6s$ state of cesium and all of the excited s, p, d, and f states up to and including $n=9$ have been calculated.[15] For reference, these oscillator strengths are given in Table

TABLE II. Calculated absorption oscillator strengths $f_{nl,n'l'}$ for cesium. The number in parentheses is the power of 10 by which the entry is to be multiplied.

Transition	$f_{nl,n'l'}$	Transition	$f_{nl,n'l'}$	Transition	$f_{nl,n'l'}$
$6s\rightarrow 6p$	1.13	$7p\rightarrow 9d$	5.93(−2)	$6d\rightarrow 9f$	1.86(−3)
$6s\rightarrow 7p$	1.13(−2)	$8p\rightarrow 9s$	4.73(−1)	$7d\rightarrow 8p$	9.08(−2)
$6p\rightarrow 8p$	1.64(−3)	$8p\rightarrow 8d$	7.48(−1)	$7d\rightarrow 9p$	1.84(−2)
$6s\rightarrow 9p$	5.0(−4)	$8p\rightarrow 9d$	1.67(−1)	$7d\rightarrow 5f$	1.49
$7s\rightarrow 7p$	1.58	$9p\rightarrow 9d$	8.00(−1)	$7d\rightarrow 6f$	2.91(−2)
$7s\rightarrow 8p$	2.80(−2)	$5d\rightarrow 7p$	1.01(−3)	$7d\rightarrow 7f$	1.97(−3)
$7s\rightarrow 9p$	4.82(−3)	$5d\rightarrow 8p$	4(−5)	$7d\rightarrow 8f$	1.20(−4)
$8s\rightarrow 8p$	2.01	$5d\rightarrow 9p$	3(−6)	$7d\rightarrow 9f$	1.8(−7)
$8s\rightarrow 9p$	4.54(−2)	$5d\rightarrow 4f$	1.79(−1)	$8d\rightarrow 9p$	1.29(−1)
$9s\rightarrow 9p$	2.44	$5d\rightarrow 5f$	8.02(−2)	$8d\rightarrow 6f$	1.79
$6p\rightarrow 7s$	1.96(−1)	$5d\rightarrow 6f$	4.31(−2)	$8d\rightarrow 7f$	6.16(−2)
$6p\rightarrow 8s$	1.94(−2)	$5d\rightarrow 7f$	2.60(−2)	$8d\rightarrow 8f$	9.26(−3)
$6p\rightarrow 9s$	6.37(−3)	$5d\rightarrow 8f$	1.69(−2)	$8d\rightarrow 9f$	2.42(−3)
$6p\rightarrow 5d$	1.03(−2)	$5d\rightarrow 9f$	1.17(−2)	$9d\rightarrow 7f$	2.06
$6p\rightarrow 6d$	6.71(−1)	$6d\rightarrow 7p$	4.87(−2)	$9d\rightarrow 8f$	9.12(−2)
$6p\rightarrow 7d$	1.28(−1)	$6d\rightarrow 8p$	8.16(−3)	$9d\rightarrow 9f$	1.74(−2)
$6p\rightarrow 8d$	4.79(−2)	$6d\rightarrow 9p$	1.55(−3)	$4f\rightarrow 7d$	1.86(−1)
$6p\rightarrow 9d$	2.38(−2)	$6d\rightarrow 4f$	1.10	$4f\rightarrow 8d$	7.55(−3)
$7p\rightarrow 8s$	3.36(−1)	$6d\rightarrow 5f$	9.1(−4)	$4f\rightarrow 9d$	2.03(−3)
$7p\rightarrow 9s$	2.98(−2)	$6d\rightarrow 6f$	1.95(−3)	$5f\rightarrow 9d$	1.58(−2)
$7p\rightarrow 7d$	7.04(−1)	$6d\rightarrow 7f$	2.63(−3)	$6d\rightarrow 9d$	5.72(−1)
$7p\rightarrow 8d$	1.51(−1)	$6d\rightarrow 8f$	2.31(−3)		

TABLE III. Comparison of discrete oscillator strengths $f_{nl,n'l'}$ for cesium. The results of our calculations are compared with experimental (columns with asterisk) and semiempirical results. The number in parentheses is the power of 10 by which the entry is to be multiplied.

Transition	This work	Ref. 16	Ref. 17	Ref. 18	Ref. 19	Ref. 20	Ref. 21
$6s\rightarrow 6p$	1.13	1.05		1.07		1.05	1.09
$6s\rightarrow 7p$	1.13(−2)	1.48(−2)	1.42(−2)	1.65(−2)	1.65(−2)	1.27(−2)	1.25(−2)
$6s\rightarrow 8p$	1.64(−3)	1.97(−3)	1.92(−3)	2.32(−3)	3.33(−3)	1.86(−3)	1.79(−3)
$6s\rightarrow 9p$	5.01(−4)	5.53(−4)	6.50(−4)	9.93(−4)	9.93(−4)	5.55(−4)	5.36(−4)
	This work	Ref. 22					
$6p\rightarrow 9s$	6.37(−3)	1.22(−2)					
$6p\rightarrow 7d$	1.28(−1)	1.24(−1)					
$6p\rightarrow 8d$	4.79(−2)	4.67(−2)					
$6p\rightarrow 9d$	2.38(−2)	2.59(−2)					
$5d\rightarrow 6f$	4.31(−2)	7.12(−2)					
$5d\rightarrow 7f$	2.60(−2)	4.14(−2)					
$5d\rightarrow 8f$	1.69(−2)	2.52(−2)					
$5d\rightarrow 9f$	1.17(−2)	1.72(−2)					

II; their systematics shall be discussed in the following section. A variety of experimental and semiempirical results for discrete oscillator strengths in cesium have been reported[16–22] along with related results on transition rates.[23] In Table III, our calculated oscillator strengths are compared with available experimental and semiempirical values[16–22] in an effort to assess our dipole matrix elements, which are the essential ingredient of the oscillator strengths; the accuracy of the discrete dipole matrix elements should be comparable to those in the continuum. Unfortunately, only a handful of experimental oscillator strengths are available. In any case, we find that our agreement of $6s\rightarrow 6p$ with experiment is quite good (within 5%), while for the higher members of the series, the agreement is less good, being worst for $6s\rightarrow 7p$ and steadily improving for the higher transitions. Note that the dipole matrix element is negative for $6s\rightarrow 6p$ and positive for $6s\rightarrow 7p$ and higher. This change of sign of the dipole matrix element, with increasing energy, is a very general phenomenon and will be discussed further in a later section. For the purpose of this comparison, however, it is sufficient to note that the poorest agreement with experiment is found in the neighborhood of this change in sign.

TABLE IV. Comparison of lifetimes (ns) of excited states of cesium theoretical results of Ref. 23.

State	This work	Ref. 23
$7s$	56.0	48.2
$8s$	101.9	90.9
$9s$	181.7	164.3
$6p$	43.7	30.9
$7p$	186.4	142.2
$8p$	334.1	333.4
$9p$	768.6	614.0
$5d$	4720.5	1133.7
$6d$	40.7	58.3
$7d$	81.3	87.6
$8d$	134.0	139.4
$9d$	213.8	213.7

The agreement of the $6p\rightarrow nd$ oscillator strengths with experiment is seen to be quite satisfactory from Table III. The $6p\rightarrow 9s$ is seen to be off by a factor of 2 from the experimental value, but in good agreement with a previous calculation.[24] This calculation is in very good agreement for higher $6p\rightarrow ns$ transitions, which leads us to be somewhat dubious of the experimental $6p\rightarrow 9s$ value. The calculated $5d\rightarrow nf$ oscillator strengths are about 30% too small, which implies that the corresponding matrix elements are somewhat too small. This is due to the theoretical d-wave potential being too attractive (as discussed above) making the $5d$ wave function too compact, thereby decreasing the overlap with the very diffuse nf wave functions. It is expected that this will be less important for higher nd states, which is borne out by the agreement of the $6p\rightarrow nd$ oscillator strengths given in Table III.

A comparison of lifetimes of selected states with other theoretical results (which are in fairly good agreement with experiment)[23] is given in Table IV. Overall, the agreement is reasonably good, indicating that our matrix elements, and energies, are also reasonable. The greatest discrepancy is about 30%, except for the $5d$ lifetime. This is due to the sensitivity of the d-wave effective potential, as discussed above.

The overall comparison of oscillator strengths and lifetimes gives us some confidence, then, that our results are reasonable, not only in the discrete range, but in the continuum as well.

C. Spectral distribution of oscillator strength

The differential oscillator strength $df/d\epsilon$ in the continuum is simply proportional to the photoionization cross section[25]

$$\frac{df}{d(\epsilon/R)}=\frac{\sigma(\text{Mb})}{8.07}$$

with R the Rydberg energy. Using the one-electron sum rule,[15]

$$\sum_{n'} f_{nl,n'l'} + \int_0^\infty \frac{df_{nl,\epsilon l'}}{d\epsilon} d\epsilon = 1 \ . \tag{7}$$

Assuming the final discrete states in the summation of Eq. (7) are rather dense, the sum can be well approximated by an integral over dn',

$$\sum_{n'} f_{nl,n'l'} = \int_{\epsilon_0}^0 f_{nl,n'l'} dn' = \int_{\epsilon_0}^0 \frac{f_{nl,n'l'}}{d\epsilon/dn'} d\epsilon \ , \tag{8}$$

where ϵ_0 is the energy of the lowest final state, so that Eq. (7) becomes

$$\int_{\epsilon_0}^0 \frac{f_{nl,n'l'}}{d\epsilon/dn'} d\epsilon + \int_0^\infty \frac{df_{nl,n'l'}}{d\epsilon} d\epsilon = 1 \ . \tag{9}$$

This shows how to represent the differential oscillator strength in the discrete,[26] as a histogram with bases laid out about the binding energies $\epsilon_{n'l'}$, widths $d\epsilon/dn'$ (evaluated at $\epsilon_{n'l'}$), and heights of $f_{nl,n'l'}/(d\epsilon/dn')$. The top of the histogram forms a staircase which constitutes an extrapolation of the continuum and, looked at in this manner, the oscillator-strength distribution, both discrete and continuum, can be treated on the same footing.

Before presenting and discussing the oscillator-strength distributions, it is useful to discuss one of the most ubiquitous features found; the dipole matrix element passing through a zero, as a function of energy, usually called the Cooper minimum.[6,27] When these occur, the dipole matrix elements have one sign at energies above the zero, and the opposite sign below the zero. These zeros are clearly seen in the continuum. There are also *indications* of Cooper minima in the discrete, when plotted as discussed above, but one rarely finds an exact zero owing to the nature of the discrete.

It is known that the oscillator-strength distributions for any state of the hydrogen atom has no zeros in the continuum. Thus, any zeros found must be due to deviations of the wave functions from hydrogenic. It is useful to think of the dipole matrix elements from our calculations as having contributions from two regions: an inner region, close to the nucleus where the initial- and final-state wave functions are complicated, and an outer region where the potential is purely Coulomb thereby making the wave functions hydrogenic, except for a phase shift (quantum defect) induced by the inner region. Since we are dealing with excited states of large spatial extent, most of the contribution to the matrix element arises from the outer region.

As a zeroth approximation, the hydrogen initial- and final-state wave functions are viewed as "in-phase" sinusoids and, as mentioned, no zeros result. For our case, the wave functions can be looked at as sinusoids which are out of phase by the relative phase difference of the initial- and final-state wave functions. Roughly speaking, then, when this phase difference between initial discrete and final continuum state is about $\pi/2$, a zero should occur right at threshold. For larger values of the phase difference, the zero would occur above threshold, since the continuum wave function moves in towards the nucleus with increasing energy. As a corollary, it seems reasonable that for a phase difference of about $3\pi/2$, two zeros will occur in that transition, and three for $5\pi/2$. These arguments, of course, overlook the inner region entirely as well as the fact that the wave functions are not sinusoids, but they do provide a useful qualitative picture.

In our convention, all wave functions have positive slope at the nucleus. Thus, all dipole matrix elements must be positive at high enough energy where the matrix element is generated near the nucleus. The mere existence of a negative dipole matrix element, therefore, is a sure indication of a Cooper minimum since at *some* energy it must change sign. As an example, the $6s \rightarrow p$ oscillator-strength distribution $df/d\epsilon$ is shown in Fig. 2. In this case the phase difference between $6s$ and the threshold p wave is just about 0.5 (in units of π). Thus, by the above discussion, we would expect a zero right around threshold. This is just what is seen near $\epsilon = 0.1$ Ry, just above threshold. The dipole matrix element is negative below the zero and positive above it, rising to a second maximum then falling off monotonically. This behavior is typical of all of the $ns \rightarrow p$ oscillator-strength distributions in Cs; with increasing principal quantum number, the zero remains almost exactly at the same energy, the threshold value of $df/d\epsilon$ increases, and the height of the second maximum decreases. Note that for the $s \rightarrow p$ transitions, the photoionization cross section is just a constant times $df/d\epsilon$ [Eq. (6)] in the continuum region ($\epsilon > 0$), since dipole selection rules allow only a single final state for initial s states.

The oscillator-strength distributions $df/d\epsilon$ for $6p \rightarrow d$ and $7p \rightarrow d$ are shown in Fig. 3. Both show a Cooper minimum in the neighborhood of 4 Ry above threshold. The $p \rightarrow d$ minima are much further out than the $s \rightarrow p$ ones were because the threshold phase-shift difference is now about 1 (in units of π) between initial and final states.

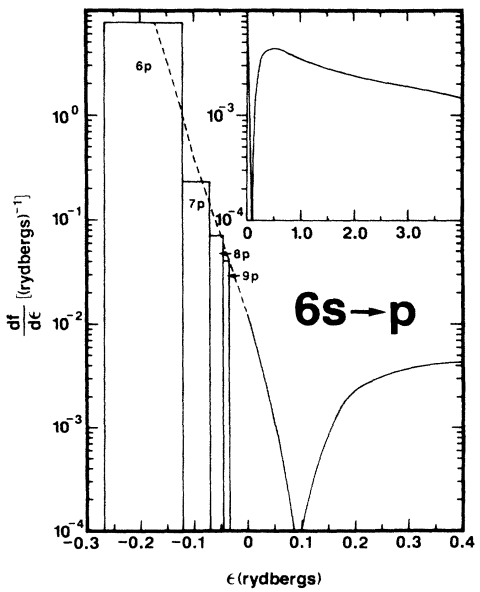

FIG. 2. Differential oscillator-strength distribution for the $6s \rightarrow p$ transitions in cesium as a function of final-state energy ϵ for both discrete ($\epsilon < 0$) and continuous ($\epsilon > 0$) spectrum.

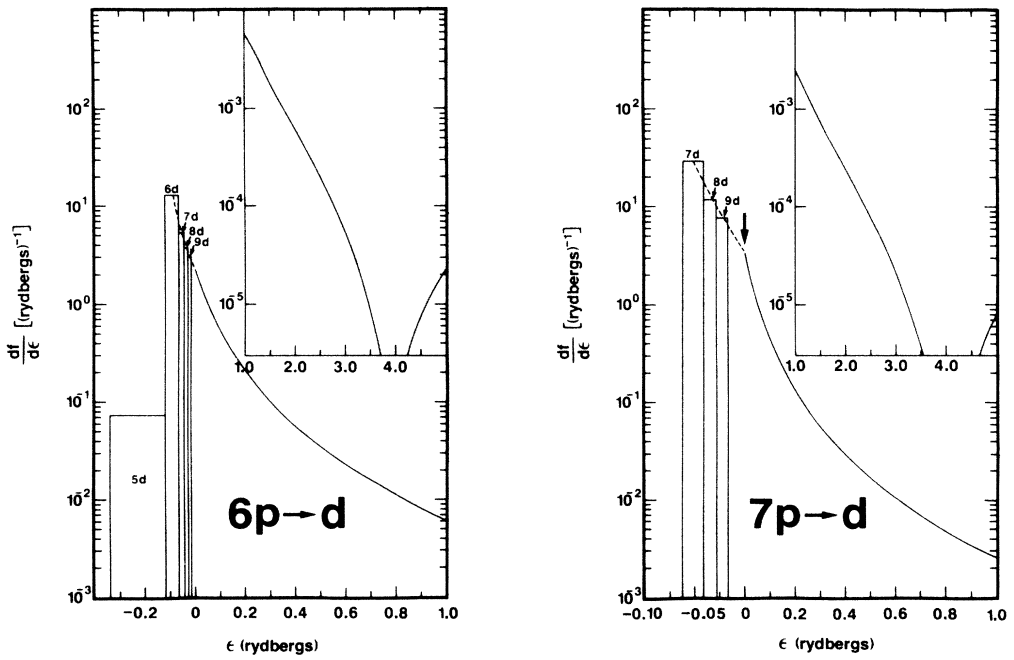

FIG. 3. Differential oscillator-strength distribution for the $6p \rightarrow d$ and $7p \rightarrow d$ transitions in cesium as a function of final-state energy ϵ for both discrete ($\epsilon < 0$) and continuous ($\epsilon > 0$) spectrum. Note the arrow indicating the change in horizontal scale.

The $p \rightarrow d$ zeros move to slightly higher energies, with increasing principal quantum number, moving 0.1 Ry in going from $6p$ to $9p$.

The $6p$ oscillator-strength distribution is slightly anomalous, compared to the other np ones, because the $6p$ lies *below* the $5d$ energy, while the higher np's all lie *above* the respective $(n-1)d$'s. Thus a break in $df/d\epsilon$ is seen for $6p$ in the discrete, but no similar break is in evidence for $7p$; there is actually a change of sign in the dipole matrix element between the $6p \rightarrow 5d$ absorption (positive) and $6p \rightarrow 6d$ (negative). Here again, however, the threshold value of $df/d\epsilon$ increases with increasing principal quantum number.

The results for $6p \rightarrow s$ are shown in Fig. 4, where it is seen that $df/d\epsilon$ is smooth with no indications of any zeros. The relative phase-shift difference at threshold is slightly below $\pi/2$, similar to the $s \rightarrow p$ case, but still no minimum results. This is due to the effect of the inner region. For the $s \rightarrow p$ transitions, increasing energy moves the ϵp wave function in toward the nucleus. This, in essence, is like an increased phase shift so that in the $s \rightarrow p$ case the phase difference can be thought of as decreasing and the zero results. For the $p \rightarrow s$ case, it is the ϵs that moves in with increasing energy, resulting in an effective increase in phase difference. When the energy increases sufficiently so that this increase is enough for the outer region to produce a zero, it is the inner region which dominates the matrix element. Thus, no zero results. This shows that there are some qualitative differences between $l \rightarrow l-1$ and $l \rightarrow l+1$ transitions. In addition, this suggests the reason that zeros in the $l \rightarrow l-1$ transitions for ground states, which are more compact to begin with, are not seen since the inner region starts to dominate at a fairly small energy.

The $nd \rightarrow f$ transitions exhibit some of the most interesting features and, therefore, all of the calculated cases are shown, in Fig. 5, rather than just a representative sample. The $5d \rightarrow f$ case shows a smooth decrease in the discrete region, then a sharp zero at $\epsilon \simeq 0.1$ Ry above threshold. The dipole matrix element is found to be posi-

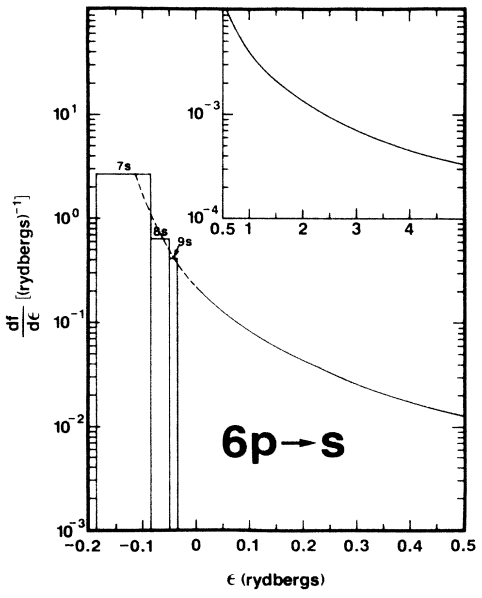

FIG. 4. Differential oscillator-strength distribution for the $6p \rightarrow s$ transitions in cesium as a function of final-state energy ϵ for both discrete ($\epsilon < 0$) and continuous ($\epsilon > 0$) spectrum.

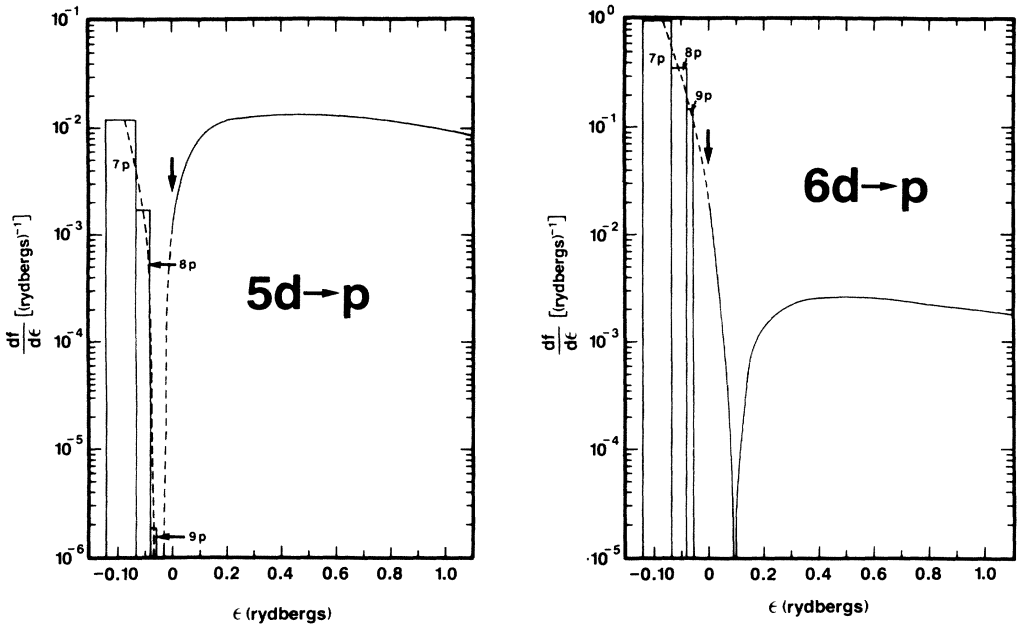

FIG. 5. Differential oscillator-strength distribution for the $nd \rightarrow f$ transitions in cesium as a function of final-state energy ϵ for both discrete ($\epsilon < 0$) and continuous ($\epsilon > 0$) spectrum. Note the arrow indicating the change in horizontal scale.

tive for the $5d \rightarrow nf$ discrete transitions. Nevertheless, a zero is seen just above threshold, where the matrix element becomes negative. By the previous discussion however, the matrix element must be positive at high enough energy. Since it is negative just above the zero shown, this means that there must be a second zero at higher energy. In fact, this is known[1] and this zero is at about 8 Ry above threshold, above the range considered in this paper.

In addition, note that the threshold phase-shift difference is just about 2.5π (cf. Fig. 1). By the arguments presented above, this large a difference would be enough to support three zeros in the dipole matrix element. The $5d$ wave function is reasonably compact, however, so that the inner region plays a role which always mitigates against zeros. This is because for small values of r, the phase shift (or quantum defect) is smaller than in the asymptotic outer region, as can be seen from a phase-amplitude analysis.[28] That is, it starts off from zero at the nucleus and accumulates value over the entire nonhydrogenic part of the potential. Thus, since smaller phase shifts (quantum defects) mean smaller phase-shift differences, it is clear that the inner region of the matrix element is more hydrogenic and, therefore, the contribution of this region makes zeros in the matrix element less likely. Then, since in the $5d \rightarrow f$ case the phase difference is about the minimum necessary to produce three zeros, the strong effect of the inner region precludes the third and only two are in evidence.

By the above discussion, for more highly excited nd states a third zero should be possible since a smaller proportion of the nd wave function is in the inner region for higher n. Looking at the $6d \rightarrow f$ in Fig. 5, it is seen that this is indeed the case; a zero appears in the discrete between $6d \rightarrow 5f$ and $6d \rightarrow 6f$. The dipole matrix element is negative for transitions to $4f$ and $5f$ and positive for the higher discrete states and the threshold continuum region. Then, about 0.1 Ry above threshold there is a zero, just like the $5d$ case, and the matrix element is negative above this point.

Going up further in n, it is seen from Fig. 5 that the zero in the continuum at about 0.1 Ry above threshold remains at a relatively constant energy as n increases. The lower energy zero, in the discrete for $6d$, moves towards higher energy with increasing n, finally moving into the continuum for the $9d \rightarrow f$ transition.[2] This upward movement is, of course, due to the decrease in importance of the inner region for more and more highly excited states, as mentioned above. The zero at much higher energy (~ 8 Ry) remains at about the same place with increasing n, also, so only the lowest energy zero is affected by increasing n.

It is worthwhile to reiterate, at this point, the fact that for orbitals bound in ground states, at most a single zero is seen for any given transition. The foregoing discussion provides the reason: ground-state orbitals are so compact that the inner region is always significant. Thus, even though the relative phase difference of initial and final states may be large enough for more than one zero, as in the case of $4d \rightarrow \epsilon f$ in Cs, the influence of the inner region precludes the possibility. The phenomenology of ground-state zeros is discussed in detail elsewhere.[29]

Note further that the three zeros in the $9d \rightarrow f$ channel are believed to be the largest number possible in any channel of any atom.[2] A fourth zero would require a minimum phase-shift difference of about 3.5π, and this large a difference does not occur for an optically allowed transition anywhere in the Periodic Table.[13]

It is evident from Fig. 5 that the existence of the zeros profoundly affects the spectral distribution of oscillator strength. Owing to the oscillator-strength sum rule (dis-

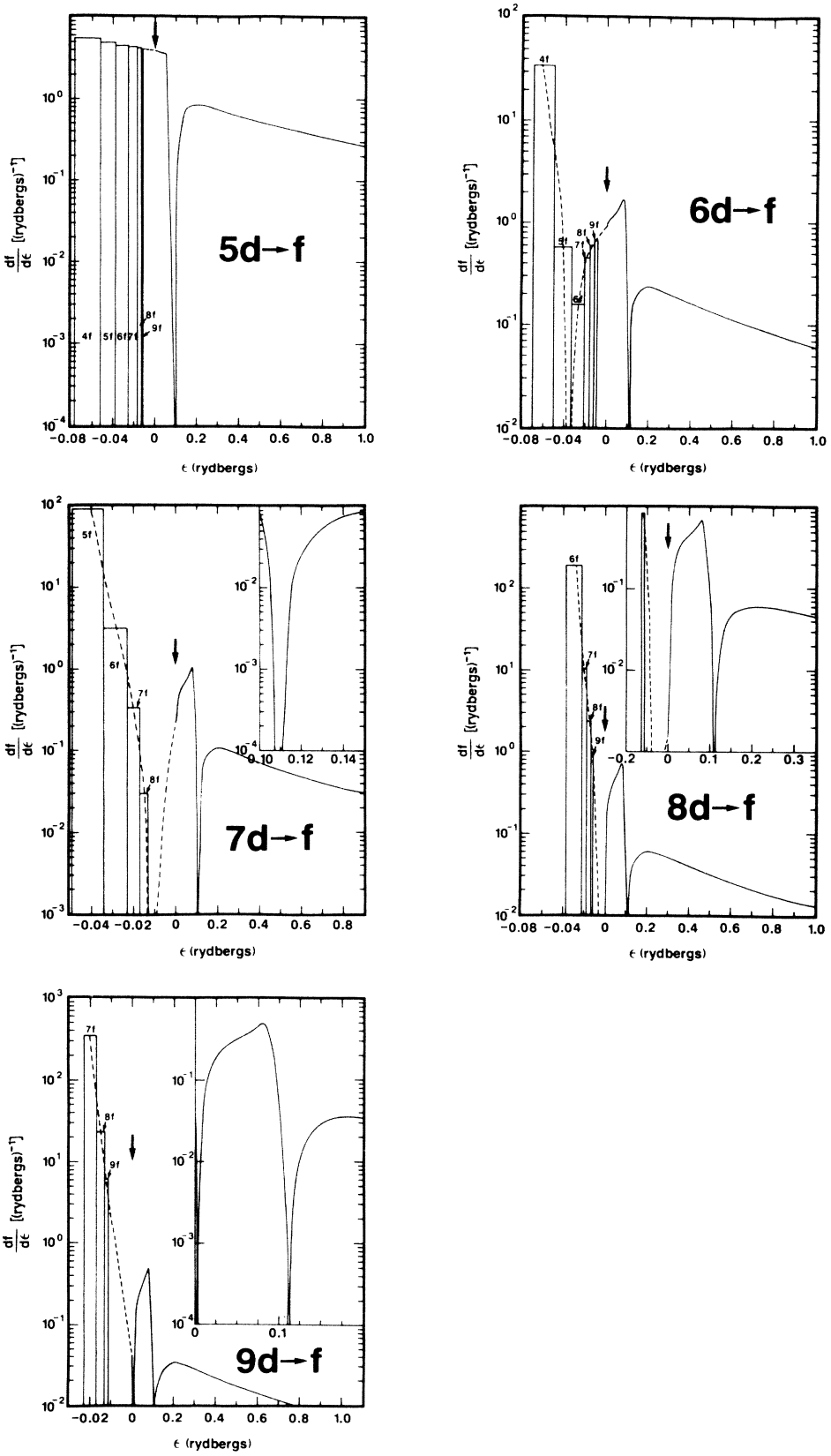

FIG. 6. Differential oscillator-strength distribution for the $5d \rightarrow p$ and $6d \rightarrow p$ transitions in cesium as a function of final-state energy ϵ for both discrete ($\epsilon < 0$) and continuous ($\epsilon > 0$) spectrum. Note the arrow indicating the change in horizontal scale.

cussed earlier), a zero in one spectral region leads to large oscillator strengths in other regions. Of course, in the continuum one looks at the photoionization cross section which is a sum of $l \rightarrow l+1$ and $l \rightarrow l-1$ contributions so that the zeros do not show up so well. This will be seen more clearly in the discussion of total subshell cross sections below.

The $nd \rightarrow p$ results are shown in Fig. 6 for $n=5$ and 6 where a zero just below the ionization threshold is seen for $5d$ and somewhat above for $6d$. The value of the phase-shift difference in these cases is about π (cf. Fig. 1) so that one zero is expected. As shown for the $nd \rightarrow f$ transitions, as n increases the effects of the inner region near the nucleus, which mitigates against there being any zeros, get increasingly less important. Thus, the zero is seen to move to higher energy in going from $5d$ to $6d$. The location of the zero is seen to dramatically alter the nature of the oscillator-strength distribution in the region of threshold. In the $5d$ case it is rapidly rising, but in the $6d$ case it is rapidly falling.

The zero continues to move to higher energy, with increasing n, as the effect of the inner region decreases, stabilizing at about 0.15 Ry above threshold for $8d \rightarrow p$ and $9d \rightarrow p$. Further, the threshold value of the differential oscillator strength increases with increasing n, as the zero moves out to higher energies. It is interesting to note, however, that although the continuum portions of the $5d \rightarrow p$ and $6d \rightarrow p$ oscillator-strength distributions are completely different, looking at the whole distribution (including the discrete range) reveals their essential similarity; the difference being whether the zero occurs below or above threshold. This point demonstrates the utility of scrutinizing the oscillator-strength distribution as a whole.

It is important to emphasize that the zeros found in the $nd \rightarrow p$ transitions are examples of zeros in $l \rightarrow l-1$ transitions. Such zeros are never found in ground-state orbitals because they are very compact with significant amplitude in the inner region. The contribution of the inner region thus precludes the existence of $l \rightarrow l-1$ zeros in ground-state orbitals. They have been shown to be a very widespread phenomenon for excited states, however.[3]

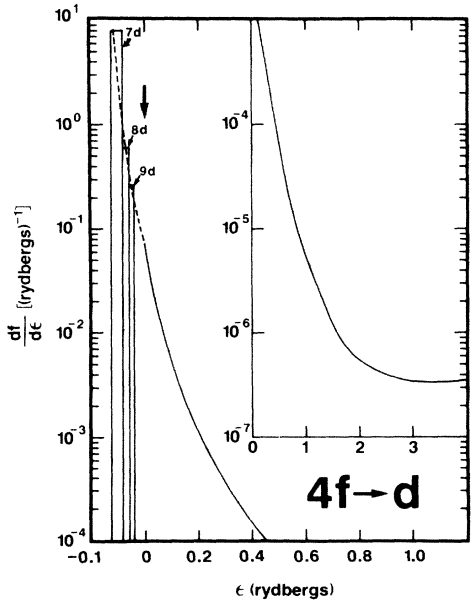

FIG. 7. Differential oscillator-strength distribution for the $4f \rightarrow d$ transitions in cesium as a function of final-state energy ϵ for both discrete ($\epsilon < 0$) and continuous ($\epsilon > 0$) spectrum. Note the arrow indicating the change in horizontal scale.

In dealing with the photoabsorption by nf states, the $nf \rightarrow g$ transitions shall not be discussed since neither the initial nor final state, in these transitions, has a quantum defect (phase shift) which appreciably differs from zero. Thus, in the energy range considered, the $nf \rightarrow g$ matrix elements are the same as for hydrogen, the properties of which are well known.[15] For the $nf \rightarrow d$ transitions, on the other hand, this is not the case as the threshold d-wave phase shift is about 2.6π, as seen in Fig. 1.

The spectral distribution of oscillator strength is given for the representative $4f \rightarrow d$ case in Fig. 7. The differential oscillator strength shows no zeros and drops monotonically from the lowest $4f \rightarrow d$ absorption. This is rather surprising as the threshold phase-shift difference is close to 2.6π. For higher n up to $9f$, the same behavior is found; no zeros and monotone decreasing. Thus, the lack of minima in Fig. 7 is not a consequence of the effect of the inner region. Why then are no zeros found? The answer lies in the energy range considered, up to 5 Ry above threshold. Sample calculations show zeros at higher energies, but the cross sections are so small above 5 Ry that the numerics become very difficult. This point shall be discussed more fully in a later publication.

D. Total subshell cross sections

The total subshell photoionization cross sections that one generally sees in an experiment are the sum of the $l \rightarrow l+1$ and $l \rightarrow l-1$ contributions. While it is possible to measure each individually using various kinds of polarized light,[30] it is still of interest to investigate the totals.

In Fig. 8, the total is shown for $6p$ along with the $6p \rightarrow d$ and $6p \rightarrow s$ partial cross sections. The pronounced zero in the $6p \rightarrow d$ channel near 4 Ry is not evident in the total owing to the strength of the $6p \rightarrow s$ channel in that region. A change of slope of the total cross section is all that is seen in the neighborhood of the zero. This demonstrates that the zero, dramatic as it is in $6p \rightarrow d$ partial cross section, can be almost totally masked in the total subshell cross section. Information on this zero can be obtained from measurements using polarized photons,[30] as mentioned above, or measurements of photoelectron angular distributions, which shall be discussed below.

Of course it is not always the case that one channel obscures features of another. As an example, the situation for $6d$ photoionization is shown in Fig. 9. Here it is seen that the $d \rightarrow p$ channel has a zero just below the sharp $d \rightarrow f$ zero. Thus, the $d \rightarrow f$ zero still shows prominently in the total subshell cross section. Over the whole energy range shown, the $d \rightarrow f$ channel dominates except near the bottom of the zero.

The total subshell cross sections for excited states with principal quantum number $n \leq 9$ and $l \leq 3$ are shown in Fig. 10. Since, as discussed in Sec. III C, the zeros occur at about the same energy for different values of n, the

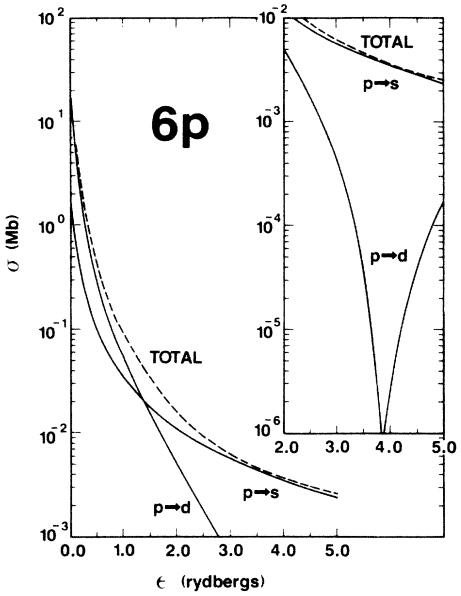

FIG. 8. Total photoionization cross section for Cs $6p$ along with the $p \rightarrow s$ and $p \rightarrow d$ partial cross sections, as a function of photoelectron energy ϵ.

cross sections are shown in a manner to make their features clear. The simplest cross sections are the nf. For these the $nf \rightarrow g$ transitions dominate in the region shown. These transitions are entirely hydrogenic, as discussed above, so that they fall monotonically from threshold. The threshold value increases and the falloff is more rapid with increasing n; the threshold cross section is about 20 Mb for $4f$ increasing to roughly 150 Mb for $9f$. The falloff scales approximately with the binding energy so that with increasing n where the binding energy decreases, the faster falloff implies a larger threshold value, since the oscillator-strength sum rule must be satisfied.

The nd cross sections are particularly interesting. Note that the minima show up very distinctly. This is because the minima are in the dominant $d \rightarrow f$ channel, coupled with the fact that there are zeros in the $d \rightarrow p$ channels quite close by as discussed in connection with $6d$, Fig. 9. They do not occur at exactly the same points, however, so that the minima in the nd cross sections do not go to zero; they are, however, very dramatic. Note that the lowest energy $9d \rightarrow f$ zero does not result in a minimum as sharp as the higher energy one, or the minima in the other nd cross sections. This is because this lowest energy $9d \rightarrow f$ zero occurs away from the $9d \rightarrow p$ minimum; thus the $9d \rightarrow p$ cross section is significant in this region and the minimum is not so dramatic. Note also that the zeros in the $nd \rightarrow p$ channels do not show up directly since the cross sections are dominated in this energy region by the $nd \rightarrow f$ channels. Their existence can be inferred from the sharpness of the minima in the nd cross sections, as explained above, as well as from photoelectron angular distributions, which will be discussed later.

The np cross sections are interesting in their simplicity; they fall monotonically from threshold. This is interesting because the $np \rightarrow d$ channels have zeros in this energy range, as seen previously. Thus, the $np \rightarrow d$ channels are anomalously small, and the cross section in the energy region shown is dominated by the $np \rightarrow s$ transitions, which were seen to have no zeros. This is shown clearly in Fig. 8 for $6p$ photoionization. Again, the existence of these zeros can be inferred from the photoelectron angular distribution, discussed below.

Finally the ns cross sections all show a zero because, for s state, only a single $ns \rightarrow p$ channel exists in each case. Thus they reflect the spectral distribution of oscillator strength for a single channel with none of their features obliterated by the addition of a second channel. Actually this is only true in a nonrelativistic calculation. Relativistic formulations allow for the possibility of $s \rightarrow p_{1/2}$ and $s \rightarrow p_{3/2}$ transitions. Since these two transitions have their zeros at *slightly* different energies, this has the effect of broadening the minimum and keeping it from going to zero.[31,32]

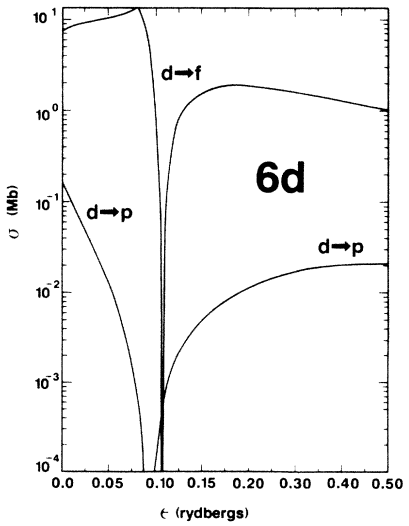

FIG. 9. Partial $d \rightarrow p$ and $d \rightarrow f$ photoionization cross sections for Cs $6d$ as a function of photoelectron energy ϵ.

E. Photoelectron angular distributions

As mentioned in the previous section, the existence of zeros can be inferred from photoelectron angular distributions. We shall not consider s states because, within our theoretical framework, Eq. (5) shows that their asymmetry parameter, $\beta=2$ and is independent of energy. The situation is otherwise for p states as exemplified by the β for $6p$ shown in Fig. 11. Here we see an energy-dependent structure in the β at low energies, which indicates both $p \rightarrow s$ and $p \rightarrow d$ channels are contributing, followed by a broad region, from 3 to 5 Ry, where β is roughly constant and equal to zero. Note the $\beta=0$ means an isotropic distribution and is indicative of the fact that the cross section is dominated in this region by the $6p \rightarrow s$ transition, an s state being isotropic. The reason it is dominated by the $6p \rightarrow s$ transition is, of course, the zero in the $6p \rightarrow d$ channel, as seen in Fig. 8. Thus, it is seen that the broad $\beta=0$ region implies a broad zero in the $6p \rightarrow d$ channel in that region; and it shows how examination of β can lead one to the existence of a zero, even though the total sub-

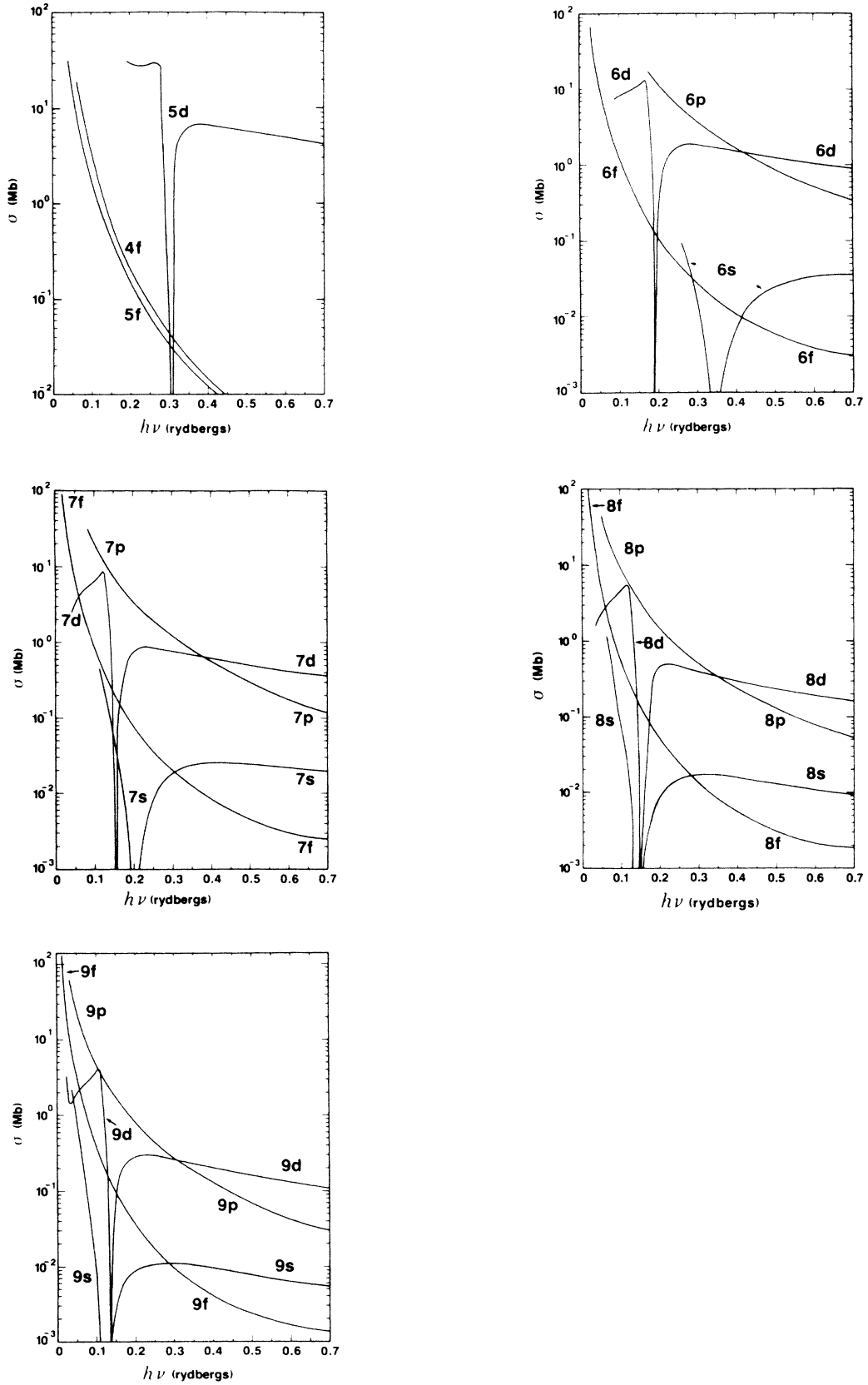

FIG. 10. Photoionization cross sections of excited states of Cs as a function of photon energy.

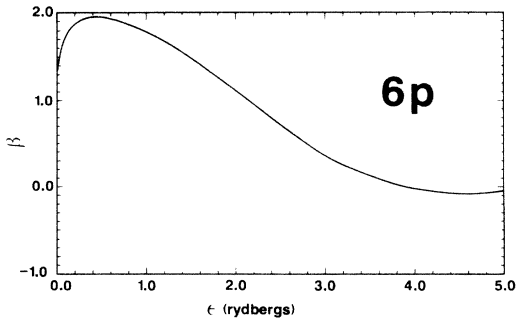

FIG. 11. Photoelectron angular distribution asymmetry parameter β for Cs $6p$ photoionization as a function of photoelectron energy ϵ.

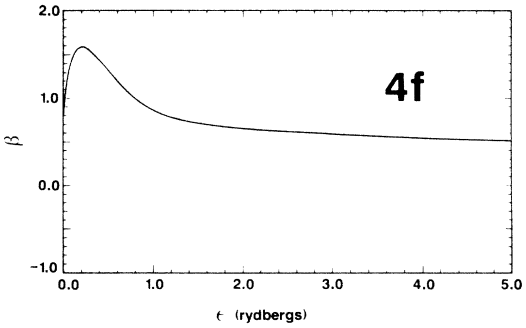

FIG. 13. Photoelectron angular distribution asymmetry parameter β for Cs $4f$ photoionization as a function of photoelectron energy ϵ.

shell cross section gives no hint of it.

A rather different β is obtained for the nd states, as seen in Fig. 12 for $6d$ photoionization. Except for the wild variation just above the 0.1 Ry, the variation of β with energy is quite slow and smooth. The wild variation is caused by the $6d \rightarrow f$ zero which causes the $6d \rightarrow f$ matrix element to change sign over a very narrow energy range. In fact, Eq. (5) shows that at the zero, $\beta = \frac{1}{5}$, which can be used to pinpoint the zero quite accurately. The resonancelike structure of β indicates that there is more than just a zero going on at that energy. The extra is a very sharp shape resonance in the ϵf channel[13] which causes not only the $d \rightarrow f$ matrix element to vary rapidly, but the phase-shift difference in Eq. (5) as well. Thus, the change in sign of the matrix element acts like a change in phase of π, and the shape resonance gives a phase change of π, for a total of 2π. This leads to a complete sinusoidal variation of one full period, which is exactly what is seen in β.

Leaving this region, it is important to note that from Eq. (5), if the dipole matrix element for the $6d \rightarrow p$ channel is negligible compared to the $6d \rightarrow f$, then $\beta = \frac{4}{5}$. Outside the resonance region (on both sides) β is never far from this value, varying only between 0.55 and 1. This indicates that outside the resonance region, the $6d \rightarrow f$ channel is quite dominant. For β to be exactly $\frac{4}{5}$, however, the $6d \rightarrow p$ matrix element would have to vanish, i.e., a zero. From Fig. 12 it is seen that this value is attained at about 0.09 Ry, indicating the presence of a $6d \rightarrow p$ zero there, just as was seen in Fig. 9.

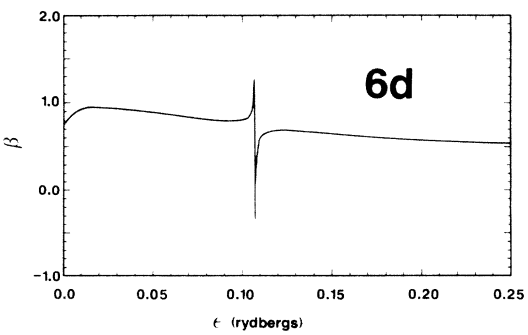

FIG. 12. Photoelectron angular distribution asymmetry parameter β for Cs $6d$ photoionization as a function of photoelectron energy ϵ.

For completeness, an example of an nf excited state, the $4f$, is shown in Fig. 13. The rise from threshold to a maximum, followed by a decline to a broad flat region, is typical of f subshells.[33] The variation in β with energy is not much affected by the variation of the matrix elements which, in this case, is very smooth. The variation is due primarily to the phase-shift difference term in Eq. (5), and primarily the Coulomb phase-shift difference which is most rapid near threshold.[33]

F. Interpolation and extrapolation of oscillator strengths

The data presented herein can be used to generate oscillator strengths from the initial states we have considered to any higher final state with $l \leq 3$ using the ideas of quantum-defect theory.[11] That this can be done reasonably can be seen from the dashed lines in the plots of the oscillator-strength distributions, Figs. 2–7. For transitions to states very close to the ionization limit, it is shown by quantum-defect theory[11] that

$$f_{nl,n'l'} \rightarrow \frac{C_{nl,l'}}{(n'^*)^3} \text{ as } n' \rightarrow \infty \ , \tag{10}$$

where $n'^* = n' - \mu_{n'l'}$, $\mu_{n'l'}$ being the final-state quantum defect and

$$C_{nl,l'} = 2 \frac{df_{nl,\epsilon l'}}{d(\epsilon/R)} \bigg|_{\epsilon=0} \ , \tag{11}$$

twice the differential oscillator strength (per unit energy in Rydbergs, R) evaluated at the ionization limit. Since $\mu_{n'l'}$ very rapidly approaches the asymptotic $\mu_{l'}$ with increasing n', it is clear that the oscillator strengths for all of the transitions of a given symmetry to very highly excited states can be obtained from the two parameters μ_l and $C_{nl,l}$; the former were given in Table I and the latter are presented in Table V.

As one moves to somewhat lower excited states, Eq. (10) is no longer quite true. But one can factor out a good deal of the variation with n by writing, in analogy with Eq. (10),

TABLE V. Theoretical results for the parameter $C_{nl,l'}$, in cesium defined by Eq. (10). Note that these are proportional to the threshold photoionization cross section of the given transition.

Transition	n = 4	5	6	7	8	9
$ns \rightarrow p$			0.0236	0.115	0.285	0.531
$np \rightarrow s$			0.439	0.827	1.292	1.827
$np \rightarrow d$			4.501	7.742	11.321	15.16
$nd \rightarrow p$		0.001 84	0.0429	0.176	0.398	0.710
$nd \rightarrow f$		7.975	1.866	0.608	0.401	0.796
$nf \rightarrow d$	0.151	0.402	0.723	1.086	1.484	1.904

$$C_{nl,n'l'} \rightarrow C_{nl,l'} \text{ as } n' \rightarrow \infty \tag{12}$$

with

$$f_{nl,n'l'} = \frac{C_{nl,n'l'}}{(n'^*)^3} \ . \tag{13}$$

In fact, as seen by Eq. (11), this $C_{nl,n'l'}$ is just twice the differential oscillator strength in the discrete as defined in Eq. (8). In any case, a knowledge of $C_{nl,nl'}$ and $\mu_{l'}$ are tantamount to a knowledge of all of the oscillator strengths in the series, except the lowest few (which have been calculated directly). The $C_{nl,n'l'} = (n'^*)^3 f_{nl,n'l'}$ are shown in Fig. 14 and can be used to find oscillator strengths not calculated directly. These curves were obtained from the calculated values of discrete oscillator strengths discussed earlier, along with the threshold continuum value at $\epsilon = 0$. The intermediate region is, thus, interpolated.

Before going on to presenting oscillator strengths obtained through this procedure, it is worthwhile to investigate the $C_{nl,n'l'}$ curves themselves. Three of the sets, $ns \rightarrow n'p$, $np \rightarrow n's$, and $nf \rightarrow n'd$, are quite smooth. Thus, the interpolation is simple and expected to be as accurate as direct calculation. Looking at $6p \rightarrow n'd$, the $nd \rightarrow n'p$, and the $nd \rightarrow n'f$ results, Cooper minima in the discrete are seen. This, of course, makes interpolation more difficult and tricky. It is seen then, that the oscillator strengths through the minimum must be obtained, along with the threshold continuum result, to perform any decent interpolation. Thus, for example, for the $6d \rightarrow n'f$ transitions, if one knew the result for $6d \rightarrow 5f$ and the threshold continuum result only, the interpolation would be completely wrong by orders of magnitude. It is therefore clear that a knowledge of the existence of these minima in the discrete is crucial to any sort of interpolation.

Turning now to using these ideas to actually obtain oscillator strengths, our results for four transitions are given in Table VI, along with various experimental results.[16,19,22] We have obtained the oscillator strengths using both the interpolation technique and Eq. (10); clearly the interpolation technique using Fig. 14 and Eq. (12) should be more accurate, but the comparison shows that they are not all that different than the results based on Eq. (10). The agreement with experiment, overall, is fairly good, especially considering the accuracy of the experimental results, e.g., for the $6s \rightarrow 12p$ transition the two experimental oscillator strengths differ by a factor of 2. In fact, comparison with Table III shows that the interpolated results are in approximately as good agreement with experiment as the oscillator strengths calculated directly. This implies that the interpolated results are as good as those calculated directly, a point we have confined by calculating some transitions to highly excited states. Thus, it is seen that the interpolation technique described above allows us to obtain a whole Rydberg series of oscillator strengths with remarkably little effort.

IV. CONCLUDING REMARKS

Calculated oscillator-strength distributions, both discrete and continuous, have been presented for a number of excited states of Cs. The outstanding feature of these results was the existence of zeros in the dipole matrix elements in discrete and continuous ranges, for both $l \rightarrow l+1$ and $l \rightarrow l-1$ transitions. Further, the existence of as many as three zeros in a single channel was found and explained in terms of relative phase shifts.

To test the accuracy of these calculations, we have com-

TABLE VI. Oscillator strengths obtained by interpolation using Eq. (10) and Eq. (12), as described in the text, compared with experiment. The number in parentheses is the power of 10 by which the entry is to be multiplied.

Transition	Eq. (12)	Eq. (10)	Experiment
$6s \rightarrow 12p$	8.72(−5)	4.68(−5)	2.41(−5),[a] 4.46(−5)[b]
$6p \rightarrow 10d$	3.09(−2)	2.53(−2)	1.66(−2)[c]
$5d \rightarrow 11f$	6.20(−3)	6.04(−3)	8.20(−3)[c]
$6p \rightarrow 13s$	7.04(−4)	6.06(−4)	1.10(−3)[c]

[a]Reference 16.
[b]Reference 19.
[c]Reference 22.

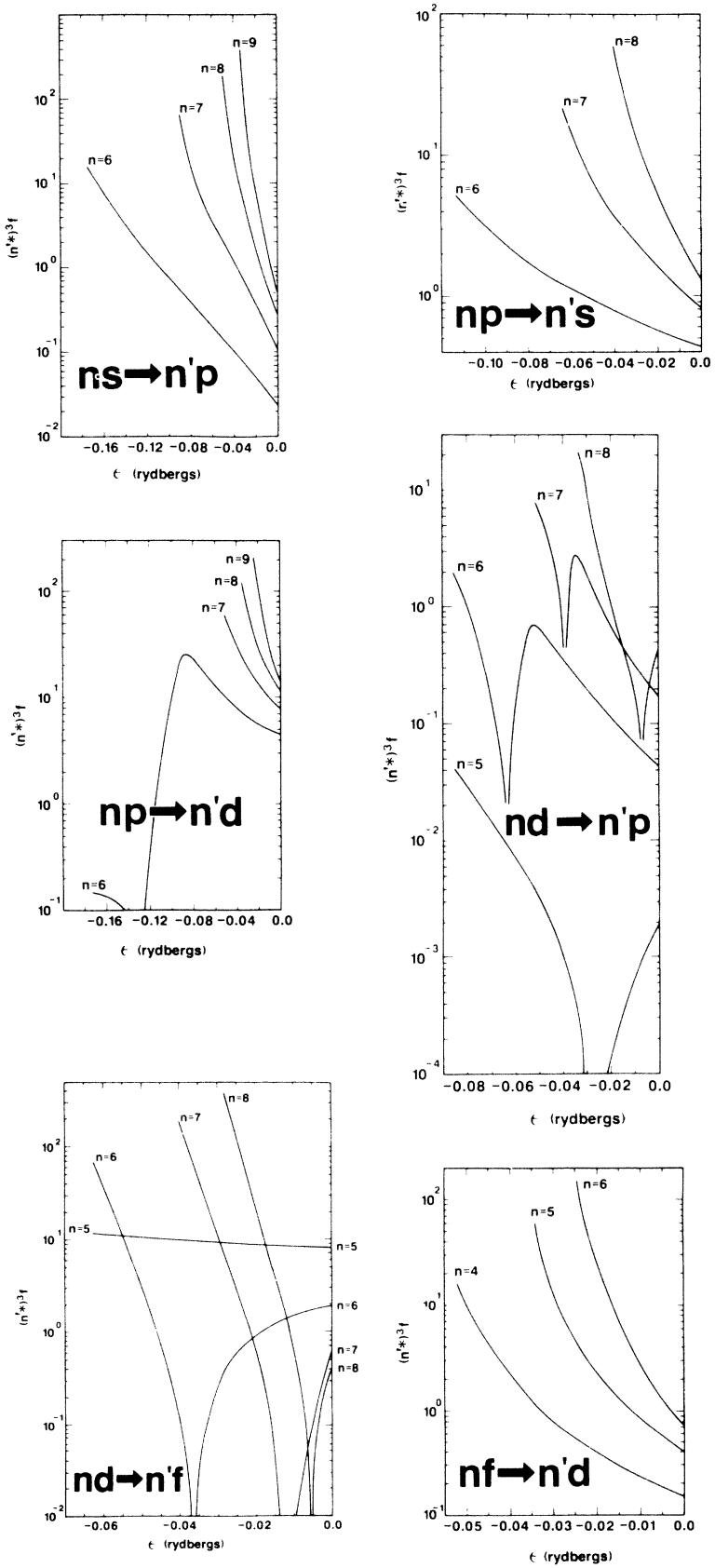

FIG. 14. The parameter $C_{nl,n'l'}=(n'^{*})^{3}f_{nl,n'l'}$ for transitions among excited states of cesium. See text for detailed explanation.

pared theoretical and experimental discrete oscillator strengths and generally found fairly good agreement. The exception was in the neighborhood of the zeros in the dipole matrix elements which, being extremely sensitive, were often somewhat off in energy. The same result was obtained in the continuum by comparing with more exact Hartree-Fock results; the minimum was shifted but the qualitative aspects of the results remained exactly the same.[4,5] In regions away from Cooper minima comparisons between theory and experiment have been made for photoionization of excited states of Na, and agreement was excellent.[34,35] Thus we conclude that our results should be fairly good quantitatively except in the region of the zeros where only qualitative accuracy is guaranteed.

Finally, we note the need for experimental data, most particularly in the continuous (photoionization) region. Some benchmark measurements are important to establish the existence and location of these various minima and to allow the predictive value of theory to be tested. Cs, with its low ionization potential, is an extremely attractive candidate for such investigations.

ACKNOWLEDGMENTS

This work was supported by the National Science Foundation and the U.S. Army Research Office.

[1]A. Z. Msezane and S. T. Manson, Phys. Rev. Lett. **35**, 364 (1975).
[2]J. Lahiri and S. T. Manson, Phys. Rev. Lett. **48**, 614 (1982).
[3]A. Z. Msezane and S. T. Manson, Phys. Rev. Lett. **48**, 473 (1982).
[4]A. Z. Msezane and S. T. Manson, Phys. Rev. A **29**, 1594 (1984).
[5]A. Z. Msezane and S. T. Manson, Phys. Rev. A **30**, 1795 (1984).
[6]A. F. Starace, in *Handbuch der Physik*, edited by W. Mehlhorn (Springer-Verlag, Berlin, 1982), Vol. 31, pp. 1–121.
[7]C. N. Yang, Phys. Rev. **74**, 764 (1948).
[8]J. Cooper and R. N. Zare, in *Lectures in Theoretical Physics*, edited by S. Geltman, K. T. Mahanthapa, and W. E. Brittin (Gordon and Breach, New York, 1969), Vol. 11-C, pp. 317–337.
[9]F. Herman and S. Skillman, *Atomic Structure Calculations* (Prentice-Hall, Englewood Cliffs, New Jersey, 1963).
[10]D. R. Bates and A. Damgaard, Philos. Trans. R. Soc. London Sec. A **242**, 101 (1949).
[11]M. J. Seaton, Proc. Phys. Soc. London **88**, 801 (1966).
[12]A. R. P. Rau and U. Fano, Phys. Rev. **167**, 7 (1968).
[13]S. T. Manson, Phys. Rev. **182**, 97 (1969).
[14]C. E. Moore, *Atomic Energy Levels*, Natl. Bur. Stand. Ref. Data Ser., Natl. Bur. Stand. (U.S.) Circ. No. 467 (U.S. GPO, Washington, D.C., 1949).
[15]H. A. Bethe and E. E. Salpeter, *Quantum Mechanics of One- and Two-Electron Atoms* (Springer-Verlag, Berlin, 1957), pp. 248–266.
[16]R. J. Exton, J. Quant. Spectrosc. Radiat. Transfer **16**, 309 (1976).
[17]G. Pichler, J. Quant. Spectrosc. Radiat. Transfer **16**, 147 (1976).
[18]M. Fabery and J. R. Cussenot, Can. J. Phys. **54**, 836 (1976).
[19]L. Agnew, Bull. Am. Phys. Soc. **11**, 327 (1966).
[20]D. W. Norcross, Phys. Rev. A **7**, 606 (1976).
[21]J. C. Weisheit, Phys. Rev. A **5**, 1621 (1972).
[22]L. Agnew and C. Summers, *Proceedings of the Seventh International Conference on Phenomena in Ionized Gases*, edited by B. Perovic and D. Tasic (Gradjevinska Knjinska, Belgrade, 1966), Vol. II, p. 574
[23]C. E. Theodosiou, Phys. Rev. A **30**, 2881 (1984).
[24]P. M. Stone, Phys. Rev. **127**, 1151 (1962).
[25]S. T. Manson and J. W. Cooper, Phys. Rev. **165**, 126 (1968).
[26]U. Fano and J. W. Cooper, Rev. Mod. Phys. **40**, 441 (1968).
[27]J. W. Cooper, Phys. Rev. **128**, 681 (1962).
[28]U. Fano, C. E. Theodosiou, and J. L. Dehmer, Rev. Mod. Phys. **48**, 49 (1976).
[29]S. T. Manson, Phys. Rev. A **31**, 3698 (1985).
[30]A. V. Smith, J. E. M. Goldsmith, D. E. Nitz, and S. J. Smith, Phys. Rev. A **22**, 577 (1980).
[31]M. J. Seaton, Proc. R. Soc. London Ser. A **208**, 418 (1951).
[32]W. Ong and S. T. Manson, Phys. Rev. A **20**, 2364 (1979).
[33]S. T. Manson, J. Electron Spectrosc. Relat. Phenom. **37**, 37 (1985).
[34]J. M. Preses, C. E. Burkhardt, R. L. Corey, D. L. Earsom, T. L. Daulton, W. P. Garver, J. J. Leventhal, A. Z. Msezane, and S. T. Manson, Phys. Rev. A **32**, 1264 (1985).
[35]A. Z. Msezane and S. T. Manson, *Abstracts of Papers, Fourteenth International Conference on the Physics of Electronic and Atomic Collisions, Palo Alto, 1985*, edited by M. J. Coggiola, D. L. Huestis, and R. P. Saxon (ICPEAC, Palo Alto, 1985), p. 21.